JOURNAL OF GUIDANCE, CONTROL, AND DYNAMICS
Vol. 20, No. 4, July–August 1997

# Near-Optimal Horizontal Trajectories for Autonomous Air Vehicles

Ilana Shapira* and Joseph Z. Ben-Asher†
*Tel-Aviv University, Tel-Aviv 69978, Israel*

**Minimum-time trajectories of unmanned aircraft in a horizontal plane are studied. The boundary conditions comprise initial and final locations and heading angles. The system model assumes instantaneously changing velocity. We view this model as a generalization of the constant-velocity model. As the study of that model has shown, the favorable trajectories that meet these boundary conditions, which have an analytical solution and comply with the minimum principle (MP), are of a bang–level–bang type. Thus, we adopt such trajectories to the current problem and investigate their compliance with the MP. The interesting result of this study is that such trajectories do not satisfy the necessary conditions of the MP inherently (as was the case in the constant velocity model), but under restrictive conditions, which are derived and analyzed. Analytic solutions are given together with some examples of the trajectories obtained. A numerical example of an optimal trajectory (with no restrictions on the number of switching points) is examined with regard to the general conditions for compliance with the MP.**

## Nomenclature

| | |
|---|---|
| $Cl_{\max}$ | = maximum lift coefficient |
| $F$ | = final location |
| $H$ | = Hamiltonian |
| $H_0$ | = the part of the Hamiltonian that is independent of the control |
| $H_1$ | = the part of the Hamiltonian that depends on the control |
| $I$ | = initial location |
| $r_m$ | = radius of turn on the bang segments |
| $t$ | = time |
| $t_f$ | = final time |
| $t_1, t_2$ | = switching times |
| $t_{21}$ | = flight time on the level flight segment |
| $u$ | = control |
| $u_1, u_2$ | = constant controls on the first and second bangs |
| $v$ | = instantaneous velocity |
| $v_b$ | = velocity along the bang segments |
| $v_m$ | = velocity along the level flight segment |
| $x_f$ | = final location on the $x$ axis |
| $x_0$ | = initial location on the $x$ axis |
| $y_f$ | = final location on the $y$ axis |
| $y_0$ | = initial location on the $y$ axis |
| $\alpha$ | = maximum rate of turn |
| $\beta$ | = velocity ratio $v_b/v_m$ |
| $\lambda_x, \lambda_y, \lambda_\psi$ | = costates |
| $\psi$ | = heading angle |
| $\psi_f$ | = final heading angle |
| $\psi_r$ | = heading angle on the level flight segment |
| $\psi_0$ | = initial heading angle |

## I. Introduction

OPTIMIZATION of atmospheric flight trajectories has been of great interest for many decades. The considerable difficulties of optimizing the exact, i.e., particle dynamics, system model resulted in approximation methods, most of which were based on the reduction of the order of the state differential system. An optimal guidance problem of a vehicle pursuing a maneuvering evader is closely related to the trajectory planning problem and has been extensively investigated. The formulation demands minimizing a weighted linear combination of the time of capture and the expended maneuvering energy (which is quadratic in the control) and thus assumes implicitly a constrained control. The singular perturbation theory[1] was used to produce feedback control laws under such an approach. The same cost function was applied to a constant-velocity interception problem with free final heading[2] and to a solution of the exact planar, nonlinear equations of motion for a guidance problem involving constant-speed vehicles.[3] A constrained control can be taken explicitly into consideration in the optimal control formulation. In this case, the cost function is the final time.[4–6] In Ref. 4, a three-dimensional time-range–optimal-turn–climb maneuver to the dash point was solved. In Ref. 5, time-optimal trajectories in the horizontal plane were studied with specific initial and final position and azimuth. Numerical solutions were derived for free final velocity and for constant velocity, indicating the existence of two boundary layers.

This work investigates time-optimal trajectories in a horizontal plane for trajectory planning purposes. The trajectories constitute solutions to a family of two-point boundary-value problems, where the initial and final locations and headings are specified and the control is limited. Systems with constant velocity and explicit constraint imposed on the control were investigated by Erzberger and Lee.[6] They showed that the trajectories are composed of a bang–bang or singular subarcs and that no optimum can contain more than three switching points, i.e., four turns. This work generalizes theirs by replacing the constant-velocity assumption with a more realistic velocity model involving an instantaneously changing velocity.[1] Such a model can be applied to air vehicles with constant throttle. This assumption is justified by the more realistic physical model of the rate of turn as a function of speed along the thrust limit. An example is shown in Fig. 1. The thrust-limit model is based on an equilibrium between thrust and drag and typically deactivates the load-factor constraints of $Cl_{\max}$ and the structural limit. Moreover, following Ref. 1, we will be using a linear curve as an approximation to the actual thrust-limit curve. Thus, solving the approximated model is a step toward the solution of the more realistic model. The solutions are limited to those that can be implemented in a real-time guidance autopilot of autonomous vehicles. Such onboard implementations may be applicable to unmanned air vehicles, whose mission is to search a given area in a given direction, to fly over certain navigation points in a specified heading, or to approach a runway or a carrier. Thus, we will confine our attention to two-switching-point trajectories of a bang–level–bang (b–l–b) type (by bang we mean applying a maximum rate of turn), which is the most common case according to Ref. 6. This choice is motivated by the recommendation in Ref. 6, by the results in Ref. 5,

Received Jan. 19, 1996; revision received Feb. 11, 1997; accepted for publication Feb. 15, 1997. 

*Graduate Student, Department of Electrical Engineering Systems.
†Adjunct Professor, Department of Electrical Engineering Systems. Member AIAA.

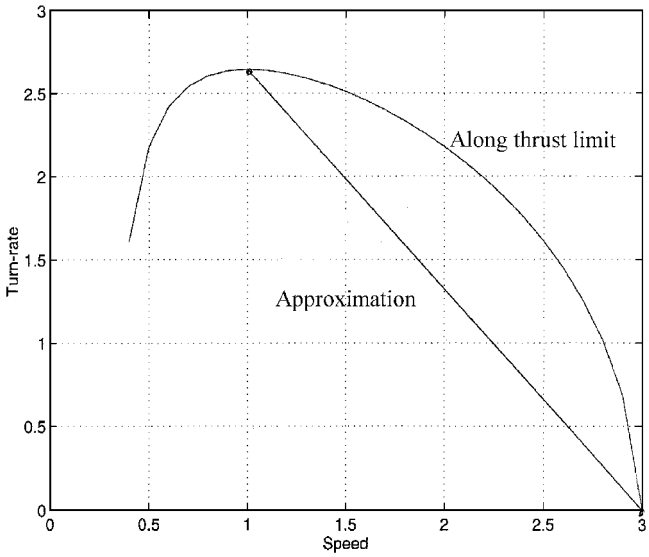


**Fig. 1 Turn rate as a function of speed for a realistic thrust-limit model and an approximated model.**

by concern for operational acceptability and simplicity, and by the insight gained from the study of constant-velocity systems.[7] It was shown that in the general case of a constant-velocity system, there are four different trajectories of this type (the number reduces to three or two in special scenarios), all of which satisfy the minimum principle (MP). Thus, it was natural to choose the same trajectories (b–l–b) for the model with instantaneously changing velocity and analyze their compliance with the MP. However, because this is a restricted family of solutions, we name these trajectories near-optimal. The minimum-time true optimal solution may or may not belong to this family. The general necessary conditions for optimality are derived, and a comparison with the constant-velocity system is carried out. An analytic solution is given, and its trajectories are presented, together with one numerical result on a time-optimal trajectory free of any restriction on the number of switching points. Finally, we note that the optimal trajectory is an open-loop one and can serve as a reference trajectory to be synthesized by proper control loops.

## II. Problem Statement

The problem concerns an air vehicle whose initial location is $I = (x_0, y_0)$ and whose heading angle is $\psi_0$. This vehicle has to get to another location $F = (x_f, y_f)$ with a heading angle $\psi_f$. The vehicle's instantaneous velocity is denoted by $v$. The problem geometry can be described, without any loss of generality, in a right-hand coordinate system whose origin is at $I$ and whose $x$ axis points in the direction of the initial heading, as shown in Fig. 2. In this coordinate system, the initial conditions $x_0 = y_0 = \psi_0 = 0$ are completely general.

This mission should be performed in minimum time, subject to a limited control constraint. The control is the rate of turn, which is typical for an aircraft, and is limited by $\alpha$. The dimensionless control is defined as the normalized rate of turn: $u = (1/\alpha)(\mathrm{d}\psi/\mathrm{d}t)$. As already stated, the velocity is assumed to be a linear function of the control magnitude[1]: $v(u) = v_m - (v_m - v_b)|u|$, as is graphically shown in Fig. 3.

It is physically reasonable that the velocity along the bang segment $v_b$, i.e., during a maximum rate of turn, should be lower than the velocity along the straight and level flight segment or during any intermediate turn. The dependence of the velocity on the control implies that the velocity is a piecewise constant function, as is the control. Such a model ignores the continuous physical time dependence of the velocity[3] for the sake of simplicity.

The equations of motion in the horizontal plane can be described in the new Cartesian coordinate system by

$$\frac{\mathrm{d}x}{\mathrm{d}t} = v(u)\cos\psi \tag{1}$$

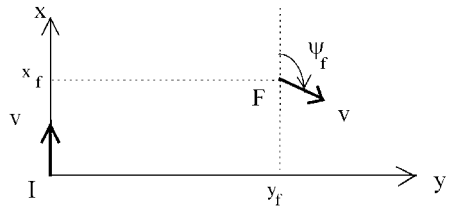


**Fig. 2 Coordinate system.**

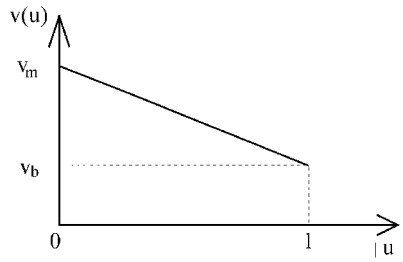


**Fig. 3 Model with instantaneously changing velocity.**

$$\frac{\mathrm{d}y}{\mathrm{d}t} = v(u)\sin\psi \tag{2}$$

$$\frac{\mathrm{d}\psi}{\mathrm{d}t} = \alpha u \tag{3}$$

with the boundary conditions

$$x(0) = y(0) = \psi(0) = 0 \tag{4}$$

$$x(t_f) = x_f \tag{5}$$

$$y(t_f) = y_f \tag{6}$$

$$\psi(t_f) = \psi_f \tag{7}$$

where $(x_f, y_f, \psi_f)$ are the final parameters in the new coordinate system. Such a problem can be solved within the framework of optimal control theory, based on the MP, where the constraint $|u| \leq 1$ is explicitly used. The solution assumes a piecewise constant control (in accordance with the basic requirements of the MP).

## III. General Formulation

The general formulation of the problem is given in Table 1. The Hamiltonian for such a formulation is smooth in the state and costate variables but not with respect to the control. Thus, the problem fits the framework of the fundamental problem as studied by Pontriyagin et al.[8]

Let us denote the velocity ratio $v_b/v_m$ by $\beta$, where $0 < \beta < 1$. The Hamiltonian contains linear terms in $u$ and $|u|$. This form reminds us of the minimum-fuel problem,[9] although there the state equations are linear in the control and the cost function is linear in the control's absolute value. The following analysis of the optimal solution will be along the same lines.

## IV. Discussion of the Optimal Control

### A. General

The Hamiltonian can be expressed as a sum of two terms, $H_0$ and $H_1(u)$. The latter depends on the control:

$$H_1(u) = A|u| + Bu$$

where

$$A = -(v_m - v_b)(c_1\cos\psi + c_2\sin\psi) \qquad B = \alpha\lambda_\psi \tag{8}$$

whereas $H_0$ is independent of the control:

$$H_0 = v_m(c_1\cos\psi + c_2\sin\psi) \tag{9}$$

Thus, $A$ is proportional to $H_0$:

$$A = -(1-\beta)H_0 \tag{10}$$

**Table 1 General formulation**

| | State equations | Initial values | Final values | Remarks |
|---|---|---|---|---|
| 1 | $\frac{dx}{dt} = v(u)\cos\psi$ | $x_0 = 0$ | $x_f$ | $v(u) = v_m - (v_m - v_b)\lvert u\rvert$ |
| 2 | $\frac{dy}{dt} = v(u)\sin\psi$ | $y_0 = 0$ | $y_f$ | |
| 3 | $\frac{d\psi}{dt} = \alpha u$ | $\psi_0 = 0$ | $\psi_f$ | $\alpha$ = maximum rate of turn |
| 4 | The cost function $J = t_f$ | | | |
| 5 | The Hamiltonian $H = \lambda_x[v_m - (v_m - v_b)\lvert u\rvert]\cos\psi + \lambda_y[v_m - (v_m - v_b)\lvert u\rvert]\sin\psi + \lambda_\psi \alpha u$ | | | |
| | Costate equations | | | Remarks |
| 6 | $\frac{d\lambda_x}{dt} = -\frac{\partial H}{\partial x} = 0$ | | | $\lambda_x$ = constant = $c_1$ |
| 7 | $\frac{d\lambda_y}{dt} = -\frac{\partial H}{\partial y} = 0$ | | | $\lambda_y$ = constant = $c_2$ |
| 8 | $\frac{d\lambda_\psi}{dt} = -\frac{\partial H}{\partial \psi}$ | | | $= [v_m - (v_m - v_b)\lvert u\rvert](c_1 \sin\psi - c_2\cos\psi)$ |
| 9 | $\frac{\partial H}{\partial u} = \begin{cases} -(v_m - v_b)(c_1\cos\psi + c_2\sin\psi) + \alpha\lambda_\psi & \text{when } u > 0 \\ (v_m - v_b)(c_1\cos\psi + c_2\sin\psi) + \alpha\lambda_\psi & \text{when } u < 0 \end{cases}$ | | | |
| 10 | The condition for a Hamiltonian that does not depend explicitly on time is $H(t) = -1$ | | | |

The sum of both terms satisfies the condition

$$H_1(u) + H_0 = -1 \tag{11}$$

The MP requires that $u$ minimize $H_1(u)$, where

$$H_1(u) = \begin{cases} (A + B)u & \text{when} \quad u \geq 0 \\ (-A + B)u & \text{when} \quad u \leq 0 \end{cases} \tag{12}$$

Note that the derivative $\partial H/\partial u$ $(= \partial H_1/\partial u)$ is not defined at $u = 0$.

The law that determines the optimal control is derived according to the dependence of $H_1(u)$ on $A$ and $B$. The control that minimizes $H_1(u)$ is given by

$$u = \begin{cases} 0 & \text{when} \quad \lvert B\rvert \leq A \\ -\text{sign}(B) & \text{when} \quad \lvert B\rvert > A \end{cases} \tag{13}$$

Two options were excluded from Eq. (13). The first option is that of $|B| = A$ and $u \neq 0$, which was found to be invalid for a finite time interval. The second option, $B = 0$ with $A \leq 0$ and $u = 1$ or $u = -1$, is also impossible, because the time derivative of $B$ when $|u| = 1$ is $v_b(c_1 \sin\psi - c_2\cos\psi)$ (see line 8 in Table 1), and this expression cannot be zero over a finite time interval, as $\psi$ is controlled by $d\psi/dt = \alpha u$ and $|u| = 1$. Thus, an optimal trajectory consists of segments with $u = 0$ or $|u| = 1$.

First we shall study the relation between $A$ and $B$ on the individual segments (this analysis is general, without any assumption on the number of switching points), and then we shall fit them to the particular b–l–b trajectories.

### B. Analysis of the Level Flight Segment ($u = 0$)

When $u = 0$, the heading angle is constant. If we denote this angle by $\psi_r$, the Hamiltonian will take the form

$$H = H_0 = v_m(c_1\cos\psi_r + c_2\sin\psi_r) = -1 \tag{14}$$

[Eq. (9)]. Consequently [Eq. (10)], $A = 1 - \beta$ is constant, whereas $B$, which is $\alpha\lambda_\psi$, is determined by

$$\frac{d\lambda_\psi}{dt} = v_m(c_1\sin\psi_r - c_2\cos\psi_r) \tag{15}$$

The slope of $\lambda_\psi$ will be adjusted to match to the values of $\lambda_\psi$ on both sides of the interval so as to provide a continuous $\lambda_\psi$.

Note that Eq. (14) implies level flight segments with two different heading angles at most in the general solution.

### C. Analysis of the Bang Segment ($|u| = 1$)

On the bang segment, $|u| = 1$. Thus, Eq. (11) can be written as

$$H = A + Bu + v_m(c_1\cos\psi + c_2\sin\psi) = -1 \tag{16}$$

where $A$ is defined in Eq. (8).

To obtain a relation between $A$ and $B$, we replace the expression $(c_1\cos\psi + c_2\sin\psi)$ in Eq. (16) with $-A/(v_m - v_b)$ from Eq. (8). This yields

$$A + Bu - \frac{v_m}{v_m - v_b}A = -1$$

which directly leads to

$$B = -u\{1 - [\beta/(1 - \beta)]A\} \tag{17}$$

In the preceding subsection, it has been shown that when $\psi \to \psi_r$, $A$ attains the value $1 - \beta$ and consequently, according to Eq. (17), $B$ attains the value $-u(1 - \beta)$, where $u$ is the control on the current bang. Thus, the limits of $A$ and $B$ when $\psi \to \psi_r$ are

$$A = 1 - \beta \qquad \text{and} \qquad B = -u(1 - \beta)$$

The time derivative of $B$ (which is equal to $\alpha\, d\lambda_\psi/dt$) can be determined by using line 8 in Table 1: $dB/dt = \alpha v_b(c_1\sin\psi - c_2\cos\psi)$.

Once $c_1$ and $c_2$ are determined, $A$ and $B$ for $|u| = 1$ become known functions of $\psi$, and their matching with the MP [$u = -\text{sign}(B)$ in Eq. (13)] can be verified.

So far the analysis applies to a solution with any number of switching points once the heading-angle profile and the adjoint variables are known. In the next section, the adjoint variables are derived for the restricted b–l–b trajectories (see Sec. I for motivation), but it is important to bear in mind the applicability of the derivation to any b–l–b subtrajectory in the general solution.

## V. Calculation of Adjoint Variables for a b–l–b Trajectory

The b–l–b trajectories are discussed in Appendix A. The adjoint variables are $\lambda_x$ $(= c_1)$, $\lambda_y$ $(= c_2)$, and $\lambda_\psi$. One equation for the adjoint coefficients $c_1$ and $c_2$ of the discussed trajectory is obtained from the continuity of $\lambda_\psi$. From Eq. (17) we conclude that if the level flight segment is defined for $t_1 \leq t \leq t_2$ and if $u_1$ and $u_2$ are the constant controls on the first and second bangs, respectively, then

$$\alpha\lambda_\psi(t)_{t \to t_1^-} = (-u_1)(1 - \beta)$$

$$\alpha\lambda_\psi(t)_{t \to t_2^+} = (-u_2)(1 - \beta)$$

whereas on the level segment, $d\lambda_\psi/dt$ is constant [see Eq. (15)]. Hence,

$$(-u_2)(1 - \beta) = (-u_1)(1 - \beta) + \alpha t_{21}\frac{d\lambda_\psi}{dt} \tag{18}$$

If $u_1 = u_2$, then $d\lambda_\psi/dt$ on the level flight segment is zero, and accordingly

$$c_1\sin\psi_r - c_2\cos\psi_r = 0$$

and $B$ is constant and satisfies

$$B = \alpha\lambda_\psi = -u_1(1 - \beta)\ [= -u_2(1 - \beta)] \neq 0$$

If $u_1 = -u_2$, then $d\lambda_\psi/dt$ on the level flight segment is a constant different from zero, and accordingly $B$ is a linear function of time (along the level segment). For $(u_1, u_2) = (1, -1)$ the slope of $B$ is positive, and for $(u_1, u_2) = (-1, 1)$ the slope is negative.

An equation for $c_1$ and $c_2$ in terms of the trajectory parameters can be derived from Eqs. (15) and (18):

$$(c_1\sin\psi_r - c_2\cos\psi_r) = \frac{(u_1 - u_2)(1 - \beta)}{\alpha v_m t_{21}} \equiv p_2 \tag{19}$$

where $p_2$ represents the slope of $\lambda_\psi$ along the level flight segment. It tends to zero as $\beta$ approaches 1 or as $t_{21}$ becomes large.

The second equation for $c_1$ and $c_2$ in terms of $\psi_r$ is obtained from Eq. (14):

$$(c_1 \cos\psi_r + c_2 \sin\psi_r) = -(1/v_m) \equiv p_1 \tag{20}$$

From Eqs. (19) and (20), $c_1$ and $c_2$ are found to be

$$c_1 = p_1 \cos\psi_r + p_2 \sin\psi_r \tag{21}$$

$$c_2 = p_1 \sin\psi_r - p_2 \cos\psi_r \tag{22}$$

These expressions describe $\lambda_x\,(=c_1)$ and $\lambda_y\,(=c_2)$ in terms of $p_1$, $p_2$ (which depend on $\alpha$, $\beta$, $v_m$, $u_1$, $u_2$, and $t_{21}$) and $\psi_r$. Thus, for a given vehicle characterized by $(\alpha, \beta, v_m)$, the quantities $\lambda_x$ and $\lambda_y$ are functions of the trajectory parameters $u_1$, $u_2$, $t_{21}$, and $\psi_r$. To obtain a similar expression for the third adjoint coefficient $\lambda_\psi$, we recall that $B$ is equal to $\alpha\lambda_\psi$ and that $B$ on a bang segment is related to $A$ according to Eq. (17). $A$ is given in Eq. (8) and can be expressed in terms of the trajectory parameters by substituting $c_1$ and $c_2$ from Eqs. (21) and (22). Thus,

$$A = (1-\beta)[\cos(\psi_r - \psi) + (p_2/p_1)\sin(\psi_r - \psi)]$$

$$B = -u\{1 - \beta[\cos(\psi_r - \psi) + (p_2/p_1)\sin(\psi_r - \psi)]\}$$

where $u$ equals $u_1$ on the first bang and $u_2$ on the second bang.

These formulas for $A$ and $B$ hold along the bang segments of a b–l–b trajectory. If $u_1 = u_2$ or $\beta = 1$, then $p_2 = 0$. The results of the adjoint variables and for $A$ and $B$ are summarized in Tables 2 and 3.

## VI. Does the b–l–b Solution Satisfy the Minimum Principle?

The answer to this question depends on the correlation between the solution obtained in terms of $(u, A, B)$ and Eq. (13). In this section, we study this correlation on the different segments and derive a very simple validity condition in terms of $A$ only.

On the level segment of the trajectory where $u_1 = u_2$, we have $A = 1-\beta$, $B = (-u_1)(1-\beta)$, and $u = 0$. These conditions match the option $u = 0$ in Eq. (13) for $|B| = A$. On the level flight segment where $u_1 = -u_2$, we have $u = 0$ and $|B| < A$, and thus they also match the option $u = 0$ in Eq. (13).

On the bang segments ($|u| = 1$), the optimal solutions should match the option $u = -\text{sign}(B)$ in Eq. (13), which requires that $|B| > A$ and $u = -\text{sign}(B)$. Here $B$ is related to $A$ according to Eq. (18):

$$B = -u\{1 - [\beta/(1-\beta)]A\} \tag{23}$$

This relation complies with $u = -\text{sign}(B)$ if and only if

$$1 - [\beta/(1-\beta)]A \geq 0 \tag{24}$$

i.e.,

$$A \leq (1-\beta)/\beta \tag{25}$$

Taking the absolute values of both sides of Eq. (23) and making use of Eq. (24) yields

$$|B| = \{1 - [\beta/(1-\beta)]A\} \tag{26}$$

Hence $|B| > A$ if and only if $1 - [\beta/(1-\beta)]A \geq A$, i.e,

$$A < 1 - \beta \tag{27}$$

which is more restrictive than Eq. (25). Thus, both conditions (25) and (26) are met if $A < 1-\beta$ along the bang sections. Therefore, this inequality assures compatibility with the MP.

We can summarize the optimality conditions for a b–l–b trajectory in the following way: the level segment inherently satisfies the MP, whereas the optimality of the bang segment is guaranteed only for $u_1 = u_2$. Thus, trajectories with $u_1 = u_2$ satisfy the MP, but trajectories with $u_1 = -u_2$ do not necessarily do so. Recall that for the constant-velocity model, both trajectories (with $u_1 = u_2$ and $u_1 = -u_2$) satisfy the MP.

A detailed investigation of Eq. (27) (Ref. 7) for $u_1 = -u_2$ shows that trajectories whose arcs on both sides of $\psi_r$ are less than $\pi$ satisfy the MP, whereas for trajectories whose arcs are greater than $\pi$, inequality (27) should be checked. As a rule, the longer the length of the level flight segment, the greater the arcs that are permissible.

## VII. Numerical Examples

A vehicle is characterized by $v_m = 800$ ft/s, $\beta = 0.6$, and $\alpha = 4.58$ deg/s. Accordingly, $v_b = \beta v_m = 480$ ft/s and the radius of turn is 6000 ft.

Some b–l–b minimum-time trajectories are calculated with respect to the final locations and heading angles given in Table 4 (see the calculation procedure in Appendix B). The trajectories are shown in Fig. 4. The compliance of those trajectories with the MP can be checked in view of Eq. (13) or, equivalently, $A$ can be checked for whether it exceeds the value $0.4\,(=1-\beta)$ along the bang segments. Once $A$ attains this value, the MP is violated and the trajectory is not a candidate for the optimal one. Examination of the function $A$ has shown that only the first trajectory violates the MP. The other examples satisfy the MP, a fact that does not exclude the existence of trajectories with shorter flight time with more than two switching

**Table 2 Adjoint variables $A$ and $B$ for a trajectory with $u \equiv u_1 = u_2$**

| Coefficient | Expression | Remarks |
|---|---|---|
| $\lambda_x$ | $-(\cos\psi_r)/v_m$ | $\lambda_x = c_1$ |
| $\lambda_y$ | $-(\sin\psi_r)/v_m$ | $\lambda_y = c_2$ |
| $\lambda_\psi$ | $-(u/\alpha)\{1 - \beta\cos[\psi_r - \psi(t)]\}$ | $u = -\text{sign}(\lambda_\psi)$ |
| $A$ | $(1-\beta)\cos(\psi_r - \psi)$ | $A = 1-\beta$ if $\psi = \psi_r$ |
| $B$ | $-u\{1 - \beta\cos[\psi_r - \psi(t)]\}$ | $B = \alpha\lambda_\psi$ |
| $\lvert B\rvert$ | $1 - \beta\cos[\psi_r - \psi(t)]$ | $\lvert B\rvert \geq A$ |

**Table 4 Numerical solutions**

| Example | $x_f$, ft | $y_f$, ft | $\psi_f$, deg | $u_1$ | $u_2$ | $t_f$, s |
|---|---|---|---|---|---|---|
| 1 | 2,000 | −1,000 | 60 | 1 | −1 | 78.87 |
| 2 | 6,000 | −15,000 | 300 | 1 | | 92.34 |
| 3 | 17,000 | 0 | 270 | 1 | −1 | 43.67 |
| 4 | 18,000 | 0 | 270 | 1 | 1 | 43.25 |
| 5 | 19,000 | 0 | 270 | 1 | −1 | 43.46 |
| 6 | 8,000 | −6,000 | 170 | −1 | −1 | 133.58 |

**Table 3 Adjoint variables $A$ and $B$ for a trajectory with $u_1 = -u_2$**

| Coefficient | Expression | Remarks |
|---|---|---|
| $\lambda_x$ | $c_1 = p_1\cos\psi_r + p_2\sin\psi_r$ | $\lambda_x = c_1$ |
| $\lambda_y$ | $c_2 = p_1\sin\psi_r - p_2\cos\psi_r$ | $\lambda_y = c_2$ |
| $\lambda_\psi$ (bang sections) | $-(u/\alpha)\{1 - \beta[\cos(\psi_r - \psi) + (p_2/p_1)\sin(\psi_r - \psi)]\}$ | $p_1 = -1/v_m$<br>$p_2 = (u_1 - u_2)(1-\beta)/\alpha v_m t_{21}$ |
| $\lambda_\psi$ (level section) | Changes linearly with time between $(-u_1/\alpha)(1-\beta)$ and $(-u_2/\alpha)(1-\beta)$ | |
| $A$ | $(1-\beta)[\cos(\psi_r - \psi) + (p_2/p_1)\sin(\psi_r - \psi)]$ | $A = (1-\beta)$ if $\psi = \psi_r$ |
| $B$ | $-u\{1 - \beta[\cos(\psi_r - \psi) + (p_2/p_1)\sin(\psi_r - \psi)]\}$ | $B = \alpha\lambda_\psi$<br>$u = u_1$ or $u = u_2$ |

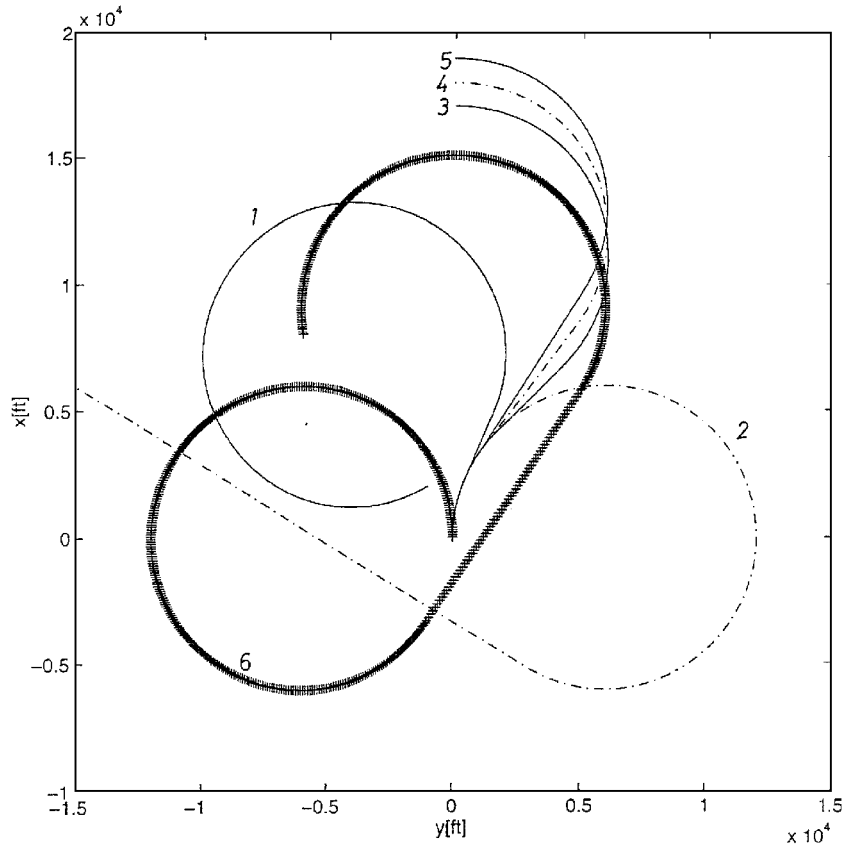


**Fig. 4 Analytical solutions for b–l–b trajectories. Trajectories of examples 1–6.**

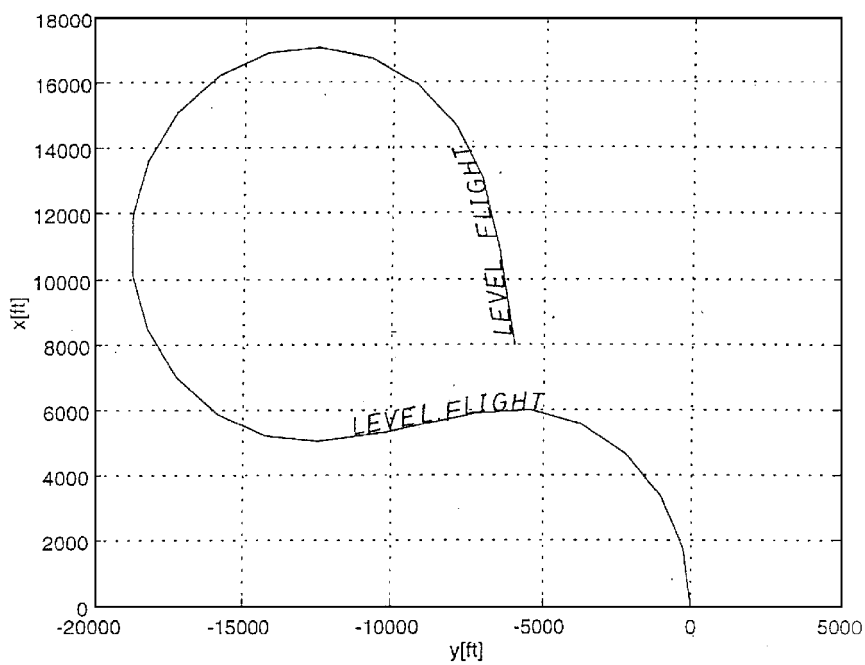


**Fig. 5 Numerical solution of a general minimum-time optimization problem.**

points or with two switching points but a structure that is not a b–l–b one.

Example 2 is a degenerate case whose second arc has vanished. Examples 3–5 demonstrate the unexpected result that it can take less time to reach a farther location (example 4 has a shorter flight time than example 3). Example 6 represents a long trajectory that results from the constraint dictated by the radius of turn (Appendix A).

Recalling the conclusion that the general solution can contain two level flight segments, an attempt has been made to look for a shorter-flight-time trajectory for example 6, expecting it to contain two level flight segments instead of one. The trajectory was obtained numerically with the help of an optimization software package, and the result is given in Fig. 5. The flight time obtained is ≈92 s (as compared to 134 s in the b–l–b case), and its function $A$ (not shown) does not exceed 0.4; hence it confirms the compliance of the trajectory with the MP [Eq. (27)]. The numerical result supports the observation that the optimal solutions contain two level flight segments at most.

## VIII. Conclusions

Time-optimal trajectories of vehicles that obey the model of instantaneously changing velocity are composed of level flight and

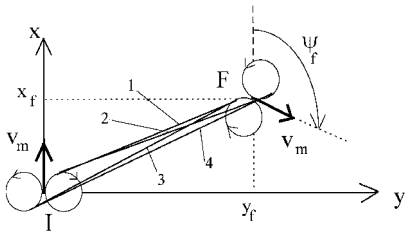


**Fig. A1 Type b–l–b trajectories.**

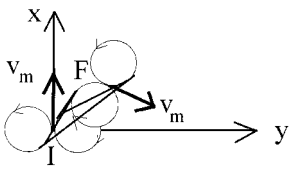


**Fig. A2 Trajectories when the motion along the overlapping circles is in the same direction.**

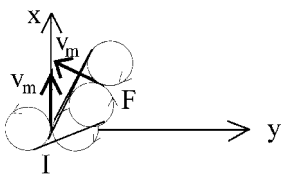


**Fig. A3 Trajectories when the motion along the overlapping circles is in opposite directions.**

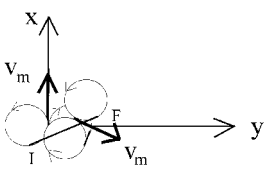


**Fig. A4 Two possible trajectories when the center of the final overlapping circle is inside the initial circle.**

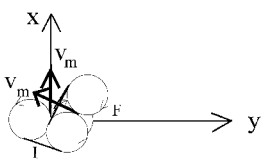


**Fig. A5 Three possible trajectories when the center of the final overlapping circle is inside the initial circle.**

bang segments, where the level flight segments are limited to two different heading angles at most. Conditions for compliance with the MP were derived for any solution given in terms of trajectory parameters and adjoint variables. The family of b–l–b trajectories was studied in detail and produced analytic expressions for the trajectories and the adjoint variables.

Applying the conditions for compliance with the MP to the analytic solution yields that trajectories with $u_1 = u_2$ satisfy the MP, whereas trajectories with $u_1 = -u_2$ satisfy the MP only when the arcs on both sides of the level segment are less than $\pi$. If the arcs are greater than $\pi$, the compliance condition should be checked. As a rule, longer level flights permit longer bang arcs. In comparison, in the constant-speed case, the MP is always satisfied by b–l–b trajectories.

The study in this paper is focused on the necessary conditions for an optimum and does not deal with the sufficient conditions. Thus, a solution that complies with the MP becomes a candidate for the time-optimal solution but is not necessarily the optimal one. Because we have used a simplified model for the rate of turn, the question arises to what extent the more realistic model (shown in Fig. 1) will affect the time-optimal solution. This question is left for a future study.

## Appendix A: B–L–B Solutions

The possible trajectories of a b–l–b type are shown in Figs. A1–A5.

1) When the range between $I$ and $F$ is sufficiently large, Fig. A1 demonstrates the four possible trajectories of a b–l–b type. Four circles are drawn in Fig. A1. Two are tangent to the initial heading at point $I$, and two are tangent to the final heading at point $F$. Trajectories 1 and 2 start at the right-hand turn circle and end on each of the final circles in the proper directions. Trajectories 3 and 4 start at the left-hand turn circle and end on each of the final circles in the proper directions.

2) When the range between $I$ and $F$ is such that one of the initial circles overlaps one of the final circles (Figs. A2 and A3), we can distinguish between two cases. In the first case, the motion along the overlapping circles is in the same direction. In this case, there is a common tangent to both circles and there are four possible trajectories, as shown in Fig. A2. In the second case, the motion

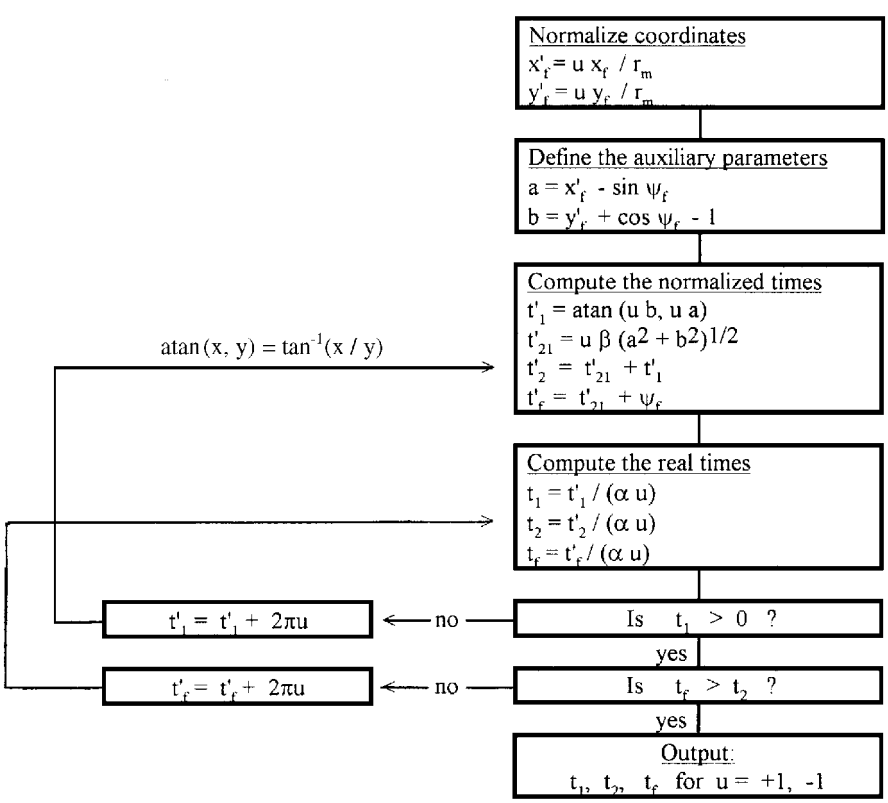


**Fig. B1 Computational procedure for $u_1 = u_2 = u$.**

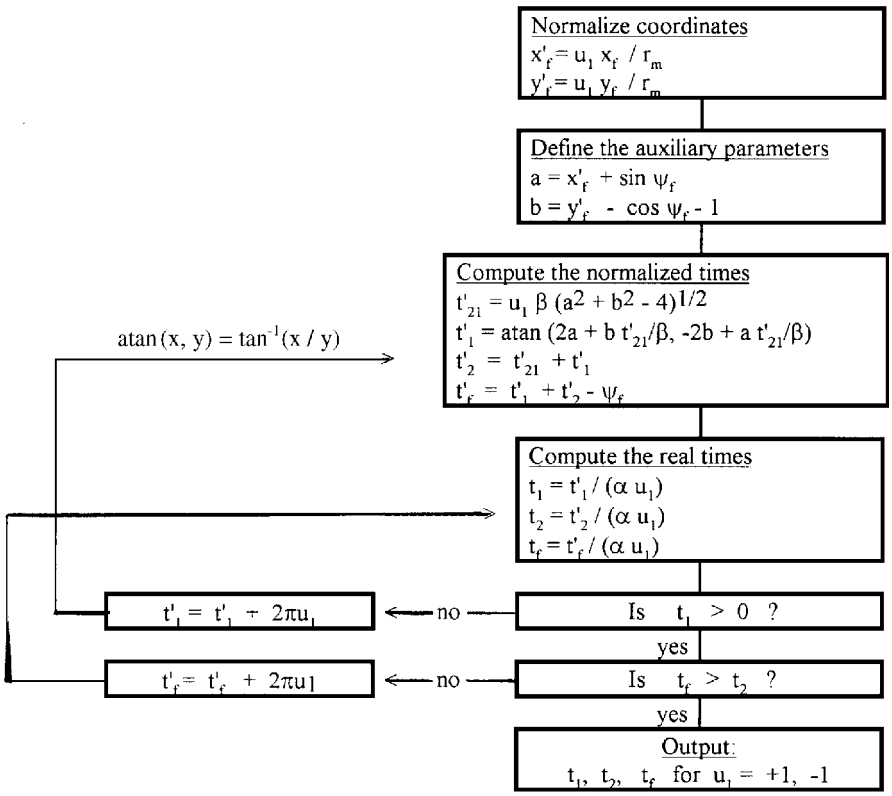


**Fig. B2 Computational procedure for $u_1 = -u_2$.**

along the overlapping circles is in opposite directions. In this case, there is no common tangent to both circles and there are only three possible trajectories, as shown in Fig. A3.

3) When point $F$ is inside one of the initial circles (Figs. A4 and A5), again two possibilities arise. If the overlapping is such that both initial circles overlap the corresponding final opposite-direction circles, then only two trajectories (those whose initial and final directions of motion are equal) are permissible (Fig. A4). If only one initial circle overlaps the final opposite-direction circle, then three trajectories are permissible (Fig. A5).

The formal solution for a b–l–b trajectory that meets the boundary conditions is carried out in Appendix B.

## Appendix B: Computational Procedure for the Switching Times

To find the minimum-time trajectory of the b–l–b type, derive the four solutions using the following four steps.

1) Given $x_f$, $y_f$, $\psi_f$, $v_m$, $\beta$, and $\alpha$, calculate $v_b = \beta v_m$, $r_m = v_b/\alpha$.

2) Solve for $u_1 = u_2$ following the procedure presented in Fig. B1 using $u_1 = +1, -1$ alternately.

3) Solve for $u_1 = -u_2$ following the procedure presented in Fig. B2 using $u_1 = +1, -1$ alternately.

4) Choose the solution that is the shortest in time.

## References

[1] Kelley, H. J., "Aircraft Maneuver Optimization by Reduced Order Approximation," *Control and Dynamic Systems*, Vol. 10, edited by C. T. Leondes, Academic, New York, 1973, pp. 131–178.

[2] Visser, H. J., and Shinar, J., "First Order Corrections in Optimal Feedback Control of Singularly Perturbed Nonlinear Systems," *IEEE Transactions on Automatic Control*, Vol. AC-31, No. 5, 1986, pp. 387–393.

[3] Guelman, M., and Shinar, J., "Optimal Guidance Law in the Plane," *Journal of Guidance, Control, and Dynamics*, Vol. 7, No. 4, 1984, pp. 471–476.

[4] Visser, H. G., Kelley, H. J., and Cliff, E. M., "Energy Management of Three-Dimensional Minimum-Time Intercept," *Journal of Guidance, Control, and Dynamics*, Vol. 10, No. 6, 1987, pp. 574–580.

[5] Ben-Asher, J. Z., "Optimal Trajectories for Unmanned Air Vehicle in the Horizontal Plane," *Journal of Aircraft*, Vol. 32, No. 3, 1995, pp. 677–680.

[6] Erzberger, H., and Lee, H. Q., "Optimum Horizontal Guidance Technique for Aircraft," *Journal of Aircraft*, Vol. 8, No. 2, 1971, pp. 95–101.

[7] Shapira, I., "2D Sub-Optimum Time Trajectories of Unmanned Aircraft," M.S. Thesis, Faculty of Electrical Engineering, Tel-Aviv Univ., Tel-Aviv, Israel, Sept. 1995.

[8] Pontryagin, L. S., Boltyanskii, V. G., Gamkrelidze, R. V., and Mishchenko, E. F., *The Mathematical Theory of Optimal Processes*, Wiley, New York, 1962, Chap. 1.

[9] Kirk, D. E., *Optimal Control Theory*, Prentice–Hall, Englewood Cliffs, NJ, 1970, Chap. 5.5.